Available online at www.sciencedirect.com
SCIENCE DIRECT®
PERGAMON
International Journal of Multiphase Flow 29 (2003) 927–941
International Journal of Multiphase Flow
www.elsevier.com/locate/ijmulflow

Numerical analysis of the continuum formulation for the initial evolution of mixing layers with particles

Djamel Lakehal *, Chidambaram Narayanan

Institute of Energy Technology, Swiss Federal Institute of Technology, ETH-Zentrum/CLT, CH-8092 Zurich, Switzerland

Received 27 October 2002; received in revised form 30 March 2003

Abstract

Numerical analysis of the standard continuum description of a dilute dispersed phase as applied to a laminar, particle-laden, mixing layer during its initial evolution has been performed. The flow has been previously analyzed under the framework of linear stability analysis where both the continuous and the dispersed phases are considered as continua. Earlier studies had neglected the closure terms resulting from the averaging of the nonlinear transport term involved in the derivation of the dispersed-phase momentum equations. In this work, Lagrangian particle tracking was coupled to an incompressible Navier–Stokes solver to directly estimate the closure terms (referred to as the averaging-stress terms) and compare them to the other terms balancing the dispersed-phase continuum equations. Calculations were performed for particle Stokes numbers of 1, 10, and 50, and for a mass loading of one. Dispersed-phase flow quantities such as the number density and velocity were determined by averaging the data in the spanwise direction. A parametric study of the influence of the number of particles, for Stokes number of one, showed that an improved approximation to a continuum can be obtained by increasing the number of particles. Examining the momentum balance in detail revealed that the main contributors were the time-derivative, convective, and the interfacial force terms. The averaging stress was at least two orders of magnitude smaller for all the Stokes numbers studied. However, the averaging stress, though negligible in magnitude, showed a deterministic variation in the center of the mixing layer. The results lend support to the currently used continuum equations for analyzing the stability of laminar, particle-laden mixing layers, and possibly other free-shear flows such as jet and wake flows.

Keywords: Continuum; Particle-laden; Mixing layer; Free shear flows; Lagrangian particle tracking

* Corresponding author. Tel.: +41-1-632-4613; fax: +41-1-632-1166.
E-mail addresses: lakehal@iet.mavt.ethz.ch (D. Lakehal), chidu@iet.mavt.ethz.ch (C. Narayanan).

0301-9322/03/$ - see front matter
doi:10.1016/S0301-9322(03)00062-4

1. Introduction

Numerical investigation and modelling of particle- and droplet-laden flows has recently evoked much interest. As a first step in analyzing fluid–particle systems, there have been several studies on the stability of laminar, particle-laden, free-shear flows to infinitesimal perturbations. Examples include mixing layers (Saffman, 1962; Yang et al., 1990; Wen and Evans, 1994, 1996; Dimas and Kiger, 1998; Tong and Wang, 1999; Narayanan and Lakehal, 2002), jets (DeSpirito and Wang, 2001), and wake flows (Yang et al., 1993) with a dilute suspension of particles. The initial evolution of such flows is described by the growth of unstable perturbations, the shape and growth rates of which could be obtained by performing a linear stability analysis of the mean velocity profile. The above studies present useful information on the inherent nature of these flows in terms of the dominant instability modes. The preferred framework in these studies has been the Eulerian continuum formulation, describing both the fluid and the particle phases as continuous media. However, some issues regarding the applicability of such a continuum formulation for these problems remain unresolved.

A detailed description of such flows includes the position and velocity information of a large number of dispersed particles, apart from the continuum (Eulerian) description of the fluid phase. Such a description is often unnecessary, apart from being beyond the reach of current and foreseeable computing capabilities. For this reason, particular attention has been paid to the description of the dispersed phase as a continuum (Reeks, 1992; Zhang and Prosperetti, 1997), where the dispersed phase is described in terms of a small number of unknowns; typical examples being the volume fraction and the average particle velocity. The derivation of continuum equations usually requires averaging, which is justified by the large number of particles present in practical flows. For example, particles with 50μ diameter occupying a volume fraction of 10^{-3} results in about 10^5 particles per cm^3.

The equations derived by averaging are not *closed*, because averaging the nonlinear convection of momentum and energy gives rise to new terms. The challenge involved in obtaining a closed set of equations by relating these terms to the average flow quantities is well known; the best illustration being the area of turbulence modelling. However, in contrast to single-phase turbulent flows where the continuum behaviour of the fluid is not in question, the averaging involved in a dispersed-phase flow operates at a more fundamental level, with the closure problem existing even in the absence of turbulence or flow unsteadiness.

This study examines, using numerical techniques, whether the neglect of the closure terms in the previously cited studies is indeed justified. For particles with nonnegligible inertia, an a priori justification for such a neglect is not available, although supporting arguments have been put forth in some cases (Zhang and Prosperetti, 1997; Dimas and Kiger, 1998; DeSpirito and Wang, 2001). The issue is examined using the Lagrangian particle tracking approach wherein the positions and velocities of individual particles are tracked. This method allows the explicit evaluation of all the terms in the the dispersed-phase mass and momentum equations by averaging, including the closure terms.

The outline of the paper is as follows. In Section 2, the continuum equations for flows laden with rigid spherical particles is presented. This is followed by a description of the Lagrangian particle tracking procedure along with its coupling to a Navier–Stokes solver. Some important

results obtained from linear stability analysis of mixing layers are then presented. The paper concludes with details of the calculations performed, followed by the results.

2. Continuum formulation for dispersed-phase flows

The commonly used equations for the linear stability analysis of flows with particles are based on "phase-averaged" quantities for both the continuous and the dispersed phases (Saffman, 1962; Dimas and Kiger, 1998). Phase average of any quantity pertaining to the continuous or dispersed phase at a point, is defined by averaging over all realizations (for ensemble averaging) in which the point is in the appropriate phase. The coupled Eulerian–Lagrangian methodology used in this study considers particles that are smaller than the significant length scales in the flow and approximates them as point masses. Therefore, calculating quantities such as the dispersed-phase number density is more natural compared to the dispersed-phase volume fraction. Consequently, an "entity-average" is used to derive the dispersed-phase equations instead of a phase average, which is retained for the continuous phase. Entity average pertains to any quantity denoting the property of a particle as a whole; examples include the center-of-mass velocity and material density. The average at a point is taken over all realizations in which a particle is centered at that point.

The use of such a hybrid averaging approach does not pose a serious problem for comparison with previous studies. If the length scale of variation (L) of the average quantities is larger than the radius of the particles (a), then the dispersed-phase volume fraction β_D, and the phase-averaged dispersed-phase velocity $\langle \mathbf{u}_D \rangle$ can be approximated by the number density n, and the center-of-mass velocity $\bar{\mathbf{w}}$ up to leading order as (Prosperetti and Zhang, 1995)

$$\beta_D = n v_p + \mathcal{O}\left(\frac{a}{L}\right)^2 \quad \text{and} \quad \langle \mathbf{u}_D \rangle = \bar{\mathbf{w}} + \mathcal{O}\left(\frac{a}{L}\right)^2, \tag{1}$$

where $v_p = 4\pi a^3/3$ is the particle volume. Therefore, we consider the dispersed-phase number density and center-of-mass velocity as approximations to the more commonly used volume fraction and phase-averaged velocity.

Such an approach, consisting of phase-averaging for the continuous phase and entity-averaging for the dispersed phase, pursued by Prosperetti and Zhang (Prosperetti and Zhang, 1995; Zhang and Prosperetti, 1997) is used as a starting point here. The main difference in this study is the use of spatial averaging along the spanwise homogeneous direction, instead of ensemble averaging in their case. Spanwise averaging is possible because the flow under consideration is two-dimensional on an average. The averaging volume can be considered to be infinite in extent in the spanwise direction, and of an arbitrary size smaller than the length scale of variation of the averaged quantities in the streamwise and vertical directions. The number of particles in the averaging volume increases with the spanwise extent and the existence of well-defined average quantities is given by the infinite spanwise extent of the averaging volume. Following the procedure in Zhang and Prosperetti (1997), we obtain the following balance equations for the continuous (assumed incompressible) and the dispersed phases:

$$\rho_{\mathrm{C}}\frac{\partial \beta_{\mathrm{C}}}{\partial t}+\rho_{\mathrm{C}}\frac{\partial}{\partial x_j}(\beta_{\mathrm{C}}\langle u_{\mathrm{C}_j}\rangle)=0, \tag{2}$$

$$\rho_{\mathrm{C}}\frac{\partial}{\partial t}(\beta_{\mathrm{C}}\langle u_{\mathrm{C}_i}\rangle)+\rho_{\mathrm{C}}\frac{\partial}{\partial x_j}(\beta_{\mathrm{C}}\langle u_{\mathrm{C}_j}\rangle\langle u_{\mathrm{C}_i}\rangle)=\frac{\partial}{\partial x_j}(\beta_{\mathrm{C}}\langle \sigma_{ij}\rangle)+\rho_{\mathrm{C}}\frac{\partial}{\partial x_j}(\beta_{\mathrm{C}}\tau_{\mathrm{C},ij})-\beta_{\mathrm{D}}f_{i,\mathrm{CD}}+\rho_{\mathrm{C}}\beta_{\mathrm{C}}g_i, \tag{3}$$

$$\rho_{\mathrm{D}}\frac{\partial n}{\partial t}+\rho_{\mathrm{D}}\frac{\partial}{\partial x_j}(n\bar{w}_j)=0, \tag{4}$$

and

$$\rho_{\mathrm{D}}\frac{\partial}{\partial t}(n\bar{w}_i)+\rho_{\mathrm{D}}\frac{\partial}{\partial x_j}(n\bar{w}_j\bar{w}_i)=\rho_{\mathrm{D}}\frac{\partial}{\partial x_j}(n\tau_{\mathrm{D},ij})+nf_{i,\mathrm{DC}}+\rho_{\mathrm{D}}ng_i, \tag{5}$$

where

$$\tau_{\mathrm{C},ij}=\langle u_{\mathrm{C}_i}\rangle\langle u_{\mathrm{C}_j}\rangle-\langle u_{\mathrm{C}_i}u_{\mathrm{C}_j}\rangle, \tag{6}$$

and

$$\tau_{\mathrm{D},ij}=\bar{w}_i\bar{w}_j-\overline{w_iw_j} \tag{7}$$

represent the unclosed stresses arising out of the averaging process. These terms will hereafter be referred to as the "averaging stresses". It must be mentioned here that these terms can arise even in the absence of flow unsteadiness and turbulence. In such a case, they represent the effect of fluid velocity fluctuations induced by the particles for the fluid phase, and the variation of the particle velocity along the spanwise direction (or within the ensemble) for the dispersed phase. Note also that the equations do not account for direct particle–particle interactions or collisions.

In the above set of equations, Eq. (2) represents the transport of the fluid volume fraction by the phase-averaged fluid velocity and Eq. (4) governs the transport of the particle number density by the entity-averaged particle velocity. Eqs. (3) and (5) govern the evolution of the phase-averaged fluid momentum and entity-averaged particle momentum, respectively. Furthermore, β_{C} denotes the continuous-phase volume fraction such that $\beta_{\mathrm{C}}+\beta_{\mathrm{D}}=1$, ρ_{C} and ρ_{D} denote the densities of the continuous and dispersed phases, respectively, that are assumed to be constants. The continuous-phase material stress tensor which consists of the pressure and the shear stresses is denoted by σ_{ij}, and the average interfacial force per unit particle volume by f_i. The interfacial force terms in the two momentum equations do not sum up to zero because of the different type of average used for each phase. Conceptually, $f_{i,\mathrm{CD}}$ is the average interfacial force due to all the interfacial surface contained inside the averaging volume, whereas $f_{i,\mathrm{DC}}$ is the average over the surface of all the particles that are centered inside the averaging volume.

The interfacial force can be approximated by that for a flow around an isolated particle for a dilute dispersed phase (Maxey and Riley, 1983; Zhang and Prosperetti, 1997). For small, rigid and heavy particles under Stokes-flow conditions, only the drag and the gravitational forces have been found to be significant (Elghobashi and Truesdell, 1992). The drag force in the Stokes flow regime can be written as

$$f_{i,\mathrm{DC}}=-9\mu(\bar{w}_i-\langle u_{\mathrm{C}_i}\rangle)/2a^2, \tag{8}$$

where μ is the fluid viscosity.

The arguments presented so far, in support of the neglect of the averaging stress terms (Eqs. (6) and (7)) are as follows: the averaging stress in the fluid would be dominated by turbulent fluctuations. For laminar flows considered in stability analyses, this term will occur only due to the disturbance velocities due to the particles. This will be quadratic in the fluid–particle relative velocity and can be neglected for dilute suspensions evolving in the Stokes-flow regime (Zhang and Prosperetti, 1997). For the dispersed-phase averaging stress, no arguments have been advanced in previous studies and the terms were neglected in the absence of a reliable option (Dimas and Kiger, 1998; DeSpirito and Wang, 2001). For particles with significant inertia that do not follow the same path as a fluid element, it is not evident that the averaging stress would be negligible.

3. Eulerian–Lagrangian method

A Lagrangian particle tracking module (Narayanan et al., 2002) was developed and coupled with an incompressible Navier–Stokes solver, to directly calculate and compare the magnitude of the averaging stress to the other terms in the dispersed-phase momentum equation. Computations were performed for the initial temporal evolution of a mixing layer with particles.

For Lagrangian particle tracking, the equations governing the particle motion are those from Maxey and Riley (1983) under the constraints outlined for Eq. (8). For compatibility with previous studies, the buoyancy force was not considered, giving

$$\frac{\mathrm{d}\mathbf{u}_\mathrm{p}}{\mathrm{d}t} = -\frac{9\mu}{2\rho_\mathrm{D} a^2}\left(\mathbf{u}_\mathrm{p} - \mathbf{u}[\mathbf{x}_\mathrm{p}(t)]\right), \tag{9}$$

where $\mathbf{u}_\mathrm{p}$ is the velocity of a particle, $\mathbf{x}_\mathrm{p}$ is its position, and $\mathbf{u}$ is the velocity of the fluid interpolated onto the particle position.

The continuous phase is represented by the incompressible Navier–Stokes equations given by

$$\frac{\partial u_j}{\partial x_j} = 0, \tag{10}$$

and

$$\frac{\partial u_i}{\partial t} + u_j\frac{\partial u_i}{\partial x_j} = -\frac{1}{\rho_\mathrm{f}}\frac{\partial p}{\partial x_i} + \frac{1}{Re}\frac{\partial^2 u_i}{\partial x_j^2} + F_i^{\mathrm{fp}}, \tag{11}$$

where F_i^{fp} is the fluid–particle interaction force per unit volume. The above equations could also be derived from Eqs. (2) and (3) by assuming that the dispersed-phase is dilute ($\beta_\mathrm{D} \ll 1$ or $\beta_\mathrm{C} \approx 1$). In other words, the displacement effect of the particles is taken to be negligible. This is also a limitation imposed by the point-mass assumption inherent in the particle tracking scheme being outlined. The coupling between the fluid and the particles is achieved by projecting the force acting on each particle on to the flow grid (Narayanan et al., 2002). The fluid-particle interaction force vector $\mathbf{F}^{\mathrm{fp}}$ has the following form at a grid node 'm':

$$\mathbf{F}_m^{\mathrm{fp}} = \sum_{\alpha=1}^{N_\mathrm{p}} \frac{\rho_\mathrm{p} v_\mathrm{p}}{\rho_\mathrm{f} V_m}\mathbf{f}^\alpha W(\mathbf{x}^\alpha, \mathbf{x}^m), \tag{12}$$

where α stands for the particle index, N_p for the total number of particles in the flow, $\mathbf{f}^\alpha$ for the force on a single particle centered at $\mathbf{x}^\alpha$, and W for the projection weight of the force on to the grid

node 'm', which is calculated based on the distance of the particle from those nodes to which the particle force is attributed. V_m is the fluid volume surrounding each grid node. For reasons already discussed, the averaging stress for the continuous phase is neglected.

The Navier–Stokes solver uses a pseudo-spectral collocation method, employing Fourier modes in the streamwise and spanwise directions and Chebychev polynomials in the vertical, nonperiodic direction. The solver is specially designed to simulate a temporally evolving mixing layer where the vertical dimension, infinite in extent, is mapped onto a $[-1, 1]$ domain using an exponential mapping function. Further details of the numerical procedure can be found in Cortesi et al. (1998).

4. Stability of mixing layers with particles

To place the current study in perspective, a brief overview of the results obtained by linear stability analysis of mixing layers with a dilute suspension of particles is presented. Several studies have been conducted on this problem starting from the analytical work of Saffman (1962), to more recent studies by Dimas and Kiger (1998) and Narayanan and Lakehal (2002). All the above studies use a similar set of continuum equations to describe the continuous and the dispersed phases. Specifically, compared to the equations in Section 2, all of them neglect the averaging stresses. Even so, important results have been obtained on the effect of particles on the Kelvin–Helmholtz instability of a mixing layer. For example, Saffman (1962) showed through scaling analysis that small particles will have a destabilizing influence on the flow whereas larger particles will stabilize the flow. This implies that for a fixed mass loading, there is a particular particle size that maximizes the stabilizing influence. Dimas and Kiger (1998) presented spatial stability analysis of an inviscid mixing layer loaded uniformly with particles. They explain the attenuation of the instability growth rate by showing that particles amplify the vorticity in the braid region and reduce the vorticity in the core region, thus, acting in opposition to the Kelvin–Helmholtz instability mechanism.

Narayanan and Lakehal (2002) presented a temporal stability analysis for both uniform and nonuniform particle loadings. They showed that particles of intermediate Stokes numbers (St) interact strongly with the flow as compared to particles of small or large Stokes numbers. Stokes number was defined as the ratio of the particle inertial time scale ($\tau_p = 2\rho_D a^2/9\mu$) to the flow time scale (τ_f) defined using the mixing-layer vorticity half-thickness and velocity half-difference. The growth rate of the mixing layer instability modes versus the perturbation wave number for different Stokes numbers, for a particle mass loading of 0.5 is shown in Fig. 1. Particle mass loading is defined as the ratio of the mass of particles to the mass of the fluid phase in the flow. Apart from the overall reduction in the growth rates for all Stokes numbers shown, wave number specific behaviour is also observed. Particles with $St = 1$ have a stronger stabilizing influence on the high- and mid-wave-number range, while particles with $St = 10$ have an even influence over the whole wave number range. A significant observation is also the reduction in the most unstable wave number, because of which a mixing layer with particles would give rise to larger vortical structures that grow much slower as compared to a particle-free mixing layer. The utility of the these results rests on the appropriateness of neglecting the averaging-stress terms. The present work aims to provide heuristic evidence to support this assumption.

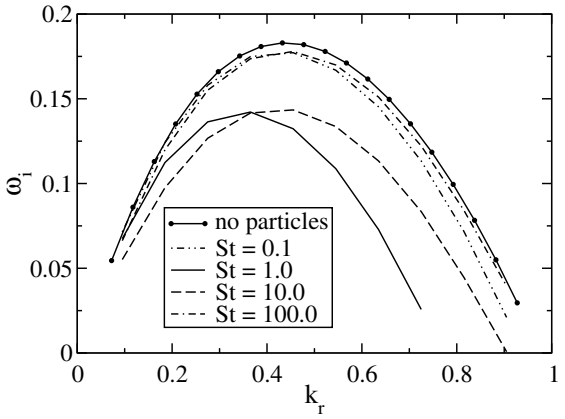

Fig. 1. Mixing layer instability growth rates versus wave number for a mass loading of 0.5.

5. Computational parameters

The mixing layer was set up using a hyperbolic-tangent streamwise velocity profile and perturbation velocities using the eigenfunctions obtained from linear stability analysis of a mixing layer uniformly laden with particles (Narayanan and Lakehal, 2002). The amplitude of the perturbations was kept small ($\leqslant 0.01$) to ensure that they evolve in the linear regime. All the quantities were nondimensionalized using the initial vorticity half-thickness as the length scale and half the velocity difference across the mixing layer as the velocity scale.

The perturbation wave number (k) was set to 0.4448, which is the most unstable wavenumber for the particle-free case (Narayanan and Lakehal, 2002). The domain size in the streamwise direction was set to $4\pi/k$. The vertical dimension for the fluid phase extended all the way up to infinity with the help of an exponential mapping. The dispersed phase was introduced between $[-8, 8]$. The spanwise dimension of the domain was chosen based on the number of particles tracked. Computations were performed with 64 collocation points in the streamwise direction and 129 points in the vertical direction for a flow Reynolds number of 250. The number of points in the spanwise direction was set based on the spanwise extent of the domain.

Calculations were performed for Stokes numbers of 1, 10, and 50, because the averaging stresses were expected to become significant for higher Stokes numbers. Because the mass loading was always fixed to one, the number of particles for a certain case was changed by altering the spanwise extent of the domain, and not by adjusting the volume fraction or the density of the particles. Particles were randomly distributed and were initialized to the local fluid velocity.

6. Results

The dispersed-phase number density, and velocities in the streamwise and vertical directions were determined using a spanwise average. The result is a two-dimensional dispersed-phase field. Terms in the mass and momentum balance equations (Eqs. (4) and (5)) were then calculated using finite-difference approximations for the derivatives. Two kinds of averages were calculated for

each term: average over half the domain and average over only the streamwise direction. The domain average was performed to gain sufficient statistical convergence, but was restricted to one half of the domain to avoid cancellation resulting from the antisymmetry of the mean streamwise velocity.

An important restriction in using the formulations described here is the requirement for the particle Reynolds number ($Re_p = 2\rho_f a|\mathbf{u}_p - \mathbf{u}(\mathbf{x}_p)|/\mu$) to remain small. This allows the use of the Stokes-flow approximation to calculate the interfacial interaction force and hence represents the condition for the validity of Eq. (9). It is not evident a priori, if the small Re_p assumption holds for particles with large Stokes numbers, because the local velocity difference is obtained only as part of the solution. The fact that the maximum Re_p for $St = 1$, 10, and 50 remains smaller than one for a considerable duration is confirmed in Fig. 2. This validates the Stokes-flow approximation in the initial period of evolution of the instability, for the Stokes numbers considered.

6.1. Dependency on the number of particles

For $St = 1$, the effect of the number of particles used for averaging was studied to show that the simulation methodology provides an improved approximation to a continuum by increasing the number of particles. Simulations were performed with 0.05, 0.1, 0.2, 0.4, 0.8, 1.6, and 3.2 million particles. In all the cases the volume fraction was set to 10^{-3}, and the density ratio was set to 1000. The nondimensional spanwise domain length was increased from 0.045, for the case with 0.05 million particles, to 2.18 for 3.2 million particles. The corresponding number of grid points in the spanwise direction were 4 and 128, respectively. Simulations were carried out to a nondimensional time of 10.

Smoother variation in all the terms is obtained as the number of particles increases. As an example, the interfacial force distributions in the vertical momentum equation with 0.1, 1.6, and 3.2 million particles are compared in Fig. 3(a). The distribution becomes significantly less noisy with 1.6 million particles compared to 0.1 million, and moreover, the difference between the profiles for 1.6 and 3.2 million particles is found to be small. To quantify (using a single number),

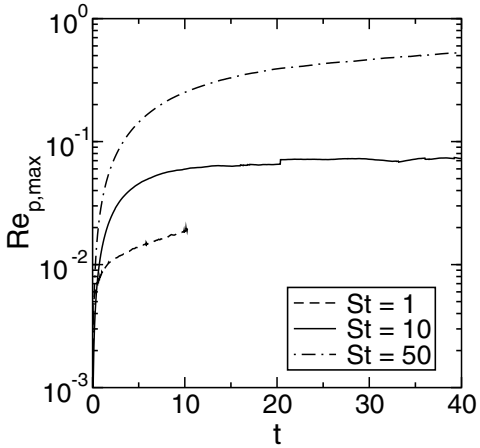

Fig. 2. Maximum particle Reynolds number variation with time.

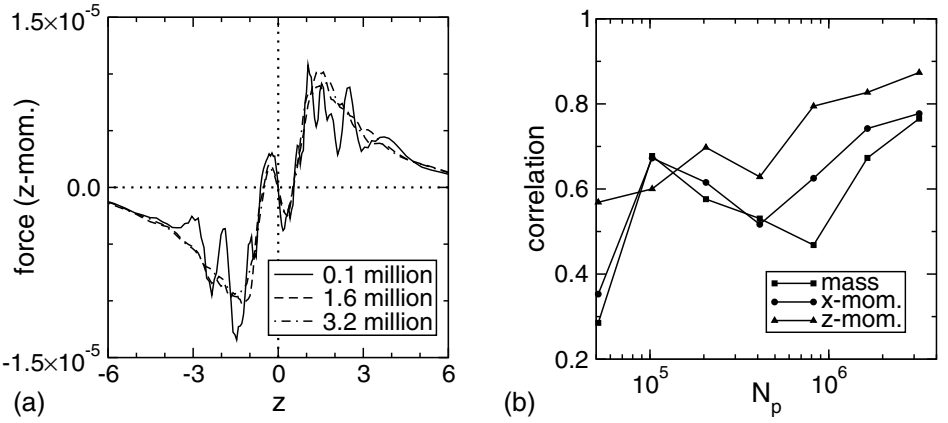

Fig. 3. (a) Variation of the interfacial force in the vertical momentum equation for different numbers of particles ($St = 1$), (b) variation of the correlation between the time-derivative and the sum of all the other terms with the number of particles.

the overall accuracy with which the balance between all the terms in the dispersed-phase momentum equation is achieved, the correlation coefficient between the time-derivative term and the sum of all the other terms was calculated. The correlation between two discrete functions f_k and g_k is defined as

$$C(f_k, g_k) = \frac{\sum_k f_k g_k}{\left(\sum_k f_k^2 \sum_k g_k^2\right)^{1/2}}. \tag{13}$$

The variation of the correlation coefficient for different numbers of particles is shown in Fig. 3(b). For streamwise averaged quantities at a nondimensional time of 10, the correlation increases with increasing number of particles for the mass as well as the momentum equations. Thus, by increasing the number of particles (through an increase in the spanwise length of the domain) the present calculation methodology provides an improving approximation to a continuum. With 3.2 million particles, the correlation for all the equations reaches values around 0.8 or more.

The simulation with 3.2 million particles for $St = 1$ is used for all subsequent analysis. For $St = 10$ and 50, such an extensive study is not feasible because the spanwise extent of the domain and the resulting number of collocation points makes it prohibitively expensive. As the motivation for this study is the examination of the relative magnitude of the terms balancing the dispersed-phase continuum equations, relevant conclusions could be drawn even without very smooth profiles. The $St = 10$ and 50 results were obtained using 0.4 and 0.2 million particles, respectively. For $St = 10$ and 50, the calculations were performed up to a nondimensional time of 40 and 60, respectively. Due to their higher inertia, these particles require more time to respond to the flow perturbations. However, extending the computation for too long makes the energy in the subharmonic mode comparable to the fundamental mode, thus, changing the nature of the problem. This criterion acts to limit the simulation time possible for higher Stokes numbers.

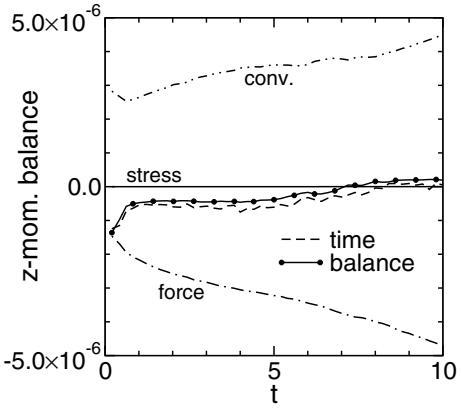

Fig. 4. Vertical momentum balance averaged over one half of the domain versus time for $St = 1$ particles.

6.2. Domain averaged results

The time evolution of the domain-averaged terms balancing the momentum equation in the vertical direction for $St = 1$ particles is shown in Fig. 4. The main balance is between the time-derivative, convective, and interfacial force terms. The averaging stress is found to be two orders of magnitude smaller than the other terms. Also, the time-derivative term and the sum of all the other terms are close to each other, showing that an overall balance is achieved. Note that the averaging-stress term is coincident with the horizontal axis in Fig. 4 as well as in some figures in the next section.

On their own, the results shown in Fig. 4 do not provide evidence for the averaging stress to be small everywhere in the domain; especially at the center of the mixing layer, which controls the dynamics of the instability evolution. Therefore, a detailed picture resulting from streamwise averaging at a particular time instant is presented below.

6.3. Streamwise averaged results

The terms balancing the streamwise momentum equation for $St = 1$ particles at a nondimensional time of 10, is shown in Fig. 5(a) and (b). Since the time-derivative term is noisier than the other terms, it is shown in a separate figure to not obscure any detail. The sum of all the other terms balancing the time-derivative term shown in Fig. 5(b) suggests that a balance between the terms is achieved. The averaging stress is found to be negligibly small even at the center of the domain. The main balance is between the time-derivative, convective, and interfacial force terms. The corresponding plots for the vertical momentum equation are presented in Fig. 6, where the averaging stress is again found to be negligible. The smoother profiles for the vertical momentum balance is consistent with the higher correlation coefficients obtained (Fig. 3(b)).

The variation of the averaging stress along the vertical direction is shown in Fig. 7 for both the streamwise and vertical momentum equations. An interesting observation is that, although the averaging stress is small, it is not exactly zero everywhere. It actually shows a deterministic

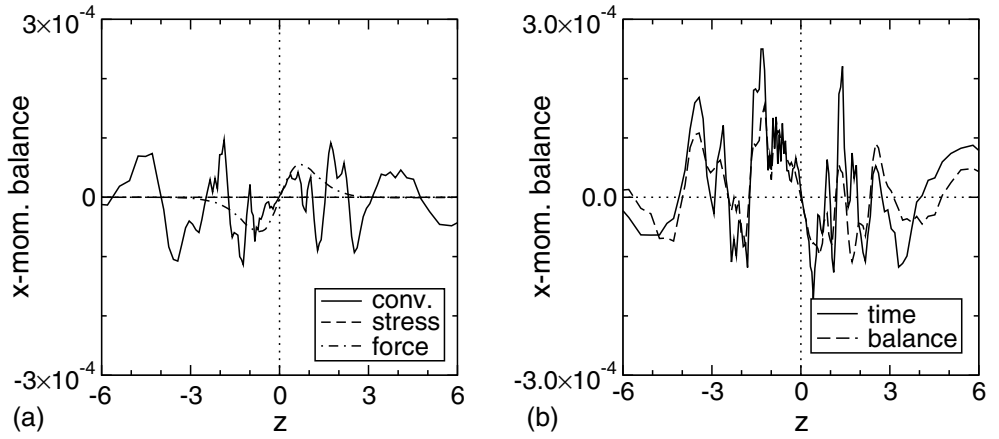

Fig. 5. Streamwise momentum balance (a) convective, averaging stress, and interfacial force, (b) time-derivative and sum of all other terms ($St = 1$).

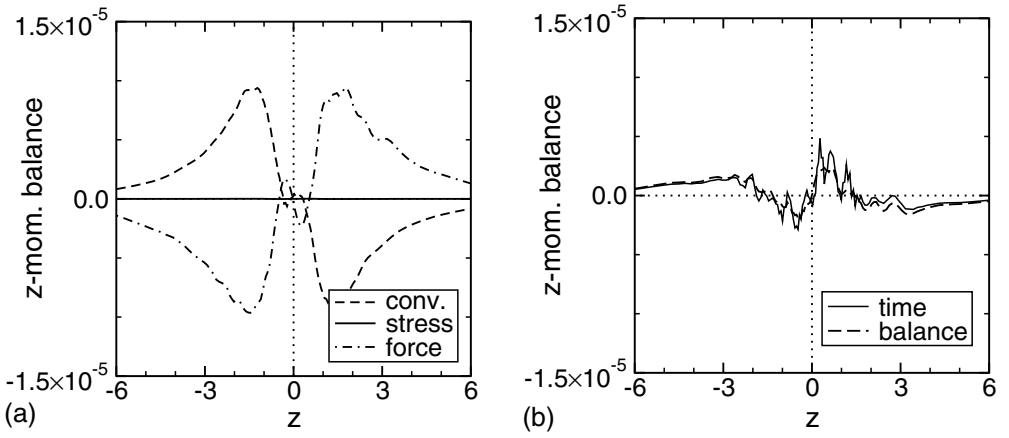

Fig. 6. Vertical momentum balance (a) convective, averaging stress, and interfacial force, (b) time-derivative and sum of all other terms ($St = 1$).

variation, especially for the vertical momentum balance. However, no attempt has been made here to examine this behaviour in more detail.

The variation of the convective, averaging stress, and interfacial force terms for the streamwise and vertical momentum equations is presented in Fig. 8 for $St = 10$ particles, and in Fig. 9 for $St = 50$ particles. The streamwise averaged quantities were calculated at a nondimensional time of 40. Without analyzing the profiles in detail, we observe that the averaging stress for both Stokes numbers is small enough to be neglected. The variation in the averaging stress shown in Fig. 10 is clearly noisier than $St = 1$ due to the smaller number of particles, however, the profiles are qualitatively similar to those for $St = 1$ particles.

In short, the averaging stress, although not precisely zero at the center of the mixing layer, can be neglected compared to the other terms in the dispersed-phase momentum equations, for the

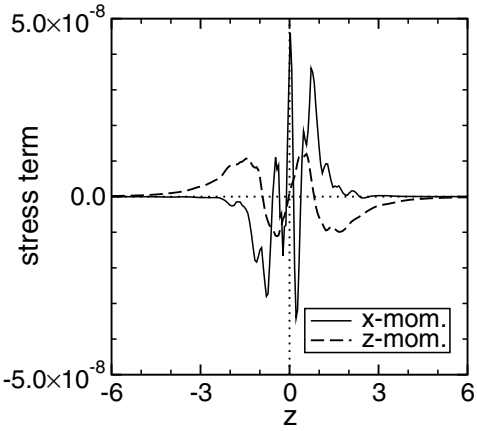

Fig. 7. Averaging stress distribution in the streamwise and vertical directions for $St = 1$ particles.

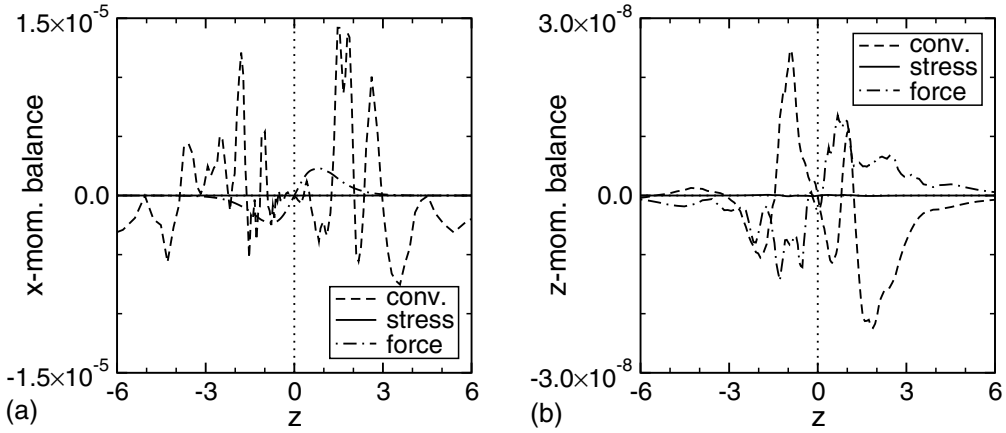

Fig. 8. Convective, averaging stress, and interfacial force terms for $St = 10$ particles: (a) streamwise momentum, (b) vertical momentum.

initial evolution of a mixing layer with particles. The results provide heuristic evidence showing the stability analyses presented in previous studies to be appropriate for the Stokes numbers considered. It remains to be seen if the same is true during the nonlinear evolution period and beyond, including the pairing of vortices and transition to turbulence. This is, however, beyond the scope of this study.

7. Conclusion

The initial evolution of mixing layers is described by the growth of unstable perturbations, the form and growth rates of which can be obtained by a linear stability analysis of the mean velocity profile. Such studies have usually used continuum equations to describe both the fluid and the

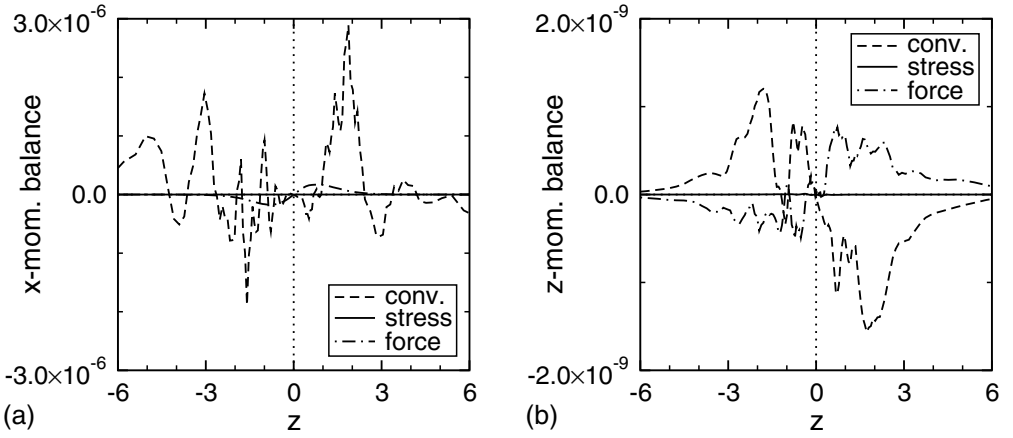

Fig. 9. Convective, averaging stress, and interfacial force terms for $St = 50$ particles: (a) streamwise momentum, (b) vertical momentum.

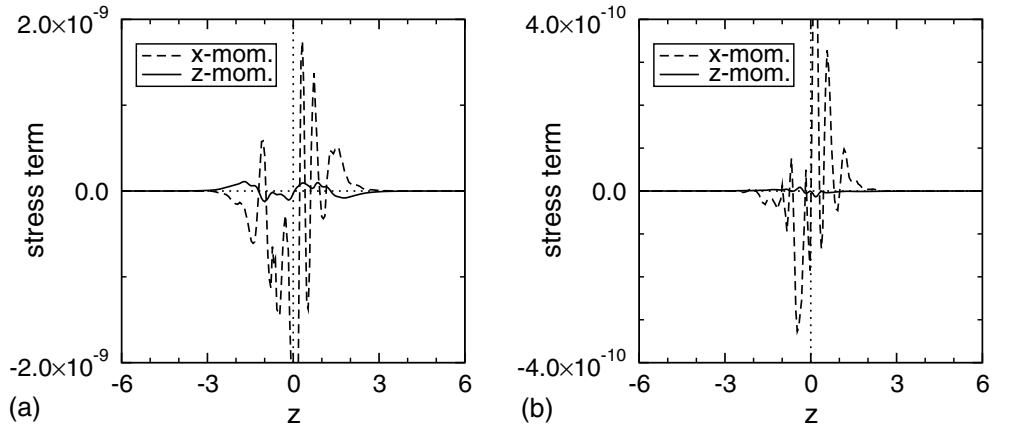

Fig. 10. Averaging stress distribution in the streamwise and vertical directions: (a) $St = 10$, (b) $St = 50$.

particle phases. The form of the continuum equations for the dispersed phase was numerically analyzed with the aid of Lagrangian particle tracking coupled to an incompressible Navier–Stokes solver. The closure terms in the dispersed-phase momentum equations were directly calculated by spatial averaging and compared to the other terms. Computations were performed for the initial temporal evolution of a mixing layer with the Stokes drag being the only interfacial force considered. Calculations were performed for Stokes numbers of 1, 10, and 50.

A parametric study of the effect of the number of particles used for averaging was performed for $St = 1$ with 0.05 to 3.2 million particles. Smoother variation in all the terms was obtained by increasing the number of particles. The overall accuracy with which the mass and momentum balance was achieved was quantified by calculating the correlation between the time-derivative term and the sum of all the other terms. The correlation showed an increasing trend with

increasing number of particles for both the mass and the momentum equations. Thus, by increasing the number of particles, an improved approximation to a continuum is obtained.

The balance between the terms averaged over one half of the domain revealed that the main contributors were the time-derivative, convective and interfacial force terms. The averaging stress was found to be two orders of magnitude smaller than the other terms. To ensure that the averaging stress is small everywhere in the domain, especially at the center of the mixing layer, the balance resulting from streamwise averaging at a particular time instant was also presented. For all the Stokes numbers, the averaging stress was found to be negligibly small, even at the center of the mixing layer. An interesting observation is that although the averaging stress term was small compared to the other terms, it was not exactly zero everywhere, and showed a deterministic variation.

Calculations were performed only for temporally evolving mixing layers, but the results could possibly apply for similar laminar free-shear flows such as jets and wakes. A logical next step would involve investigating the dispersed-phase momentum balance during the later stages in the evolution of a mixing layer with particles, including the process of vortex pairing and transition to turbulence.

Acknowledgements

The authors appreciate the support and guidance from Prof. George Yadigaroglu and would like to thank Dr. Denis Labutin from the Department of Mathematics, ETH-Zurich for his help. This work was funded by the European Research Community on Flow Turbulence and Combustion (ERCOFTAC), through the Leonhard Euler Center, Switzerland.

References

Cortesi, A.B., Yadigaroglu, G., Banerjee, S., 1998. Numerical investigation of the formation of three-dimensional structures in stably-stratified mixing layers. Phys. Fluids 10, 1449–1473.

DeSpirito, J., Wang, L.-P., 2001. Linear instability of two-way coupled particle-laden jet. Int. J. Multiphase Flow 27, 1179–1198.

Dimas, A.A., Kiger, K.T., 1998. Linear instability of a particle-laden mixing layer with a dynamic dispersed phase. Phys. Fluids 10, 2539–2557.

Elghobashi, S., Truesdell, G.C., 1992. Direct simulation of particle dispersion in a decaying isotropic turbulence. J. Fluid Mech. 242, 655–700.

Maxey, M.R., Riley, J.K., 1983. Equation of motion for a small rigid sphere in a nonuniform flow. Phys. Fluids 26, 883–889.

Narayanan, C., Lakehal, D., 2002. Temporal instabilities of a mixing layer with uniform and nonuniform particle loadings. Phys. Fluids 14, 3775–3789.

Narayanan, C., Lakehal, D., Yadigaroglu, G., 2002. Linear stability analysis of particle-laden mixing layers using Lagrangian particle tracking. Powder Technol. 125, 122–130.

Prosperetti, A., Zhang, D.Z., 1995. Finite-particle-size effects in disperse two-phase flows. Theoret. Comput. Fluid Dynam. 7, 429–440.

Reeks, M.W., 1992. On the continuum equations for dispersed particles in nonuniform flows. Phys. Fluids A 4, 1290–1303.

Saffman, P.G., 1962. On the stability of laminar flow of a dusty gas. J. Fluid Mech. 13, 120–128.

Tong, X.-L., Wang, L.-P., 1999. Two-way coupled particle-laden mixing layer. Part 1: Linear instability. Int. J. Multiphase Flow 25, 575–598.

Wen, F., Evans, J., 1994. Linear instability of a two-layer flow with differential particle loading. Phys. Fluids 6, 3893–3905.

Wen, F., Evans, J., 1996. Effect of particle inertia on the instability of a particle-laden flow. Comp. Fluids 25, 667–676.

Yang, Y., Chung, J.N., Troutt, T.R., Crowe, C.T., 1990. The influence of particles on the spatial stability of two-phase mixing layers. Phys. Fluids A 2, 1839–1845.

Yang, Y., Chung, J.N., Troutt, T.R., Crowe, C.T., 1993. The effects of particles on the stability of a two-phase wake flow. Int. J. Multiphase Flow 19, 137–149.

Zhang, D.Z., Prosperetti, A., 1997. Momentum and energy equations for disperse two-phase flow and their closure for dilute suspensions. Int. J. Multiphase Flow 23, 425–453.